1A.9

PECULIAR SUPERCELL TORNADOES CAUSED BY TYPHOON 'NEOGURI'

Soichiro Yuasa and Koji Sassa*

Dept. of applied Science, Kochi University

1. INTRODUCTION

Typhoon is one of major source of tornadoes in Japan. Some Typhoons cause mini-supercell tornadoes (Suzuki et al. 2000). Typical case is the Nobeoka tornado caused by Typhoon 'Shanshan' on 17 September 2006 (Mashiko et al. 2009). The Nobeoka tornado occurred in the outer rainband of the Typhoon 'Shanshan'.

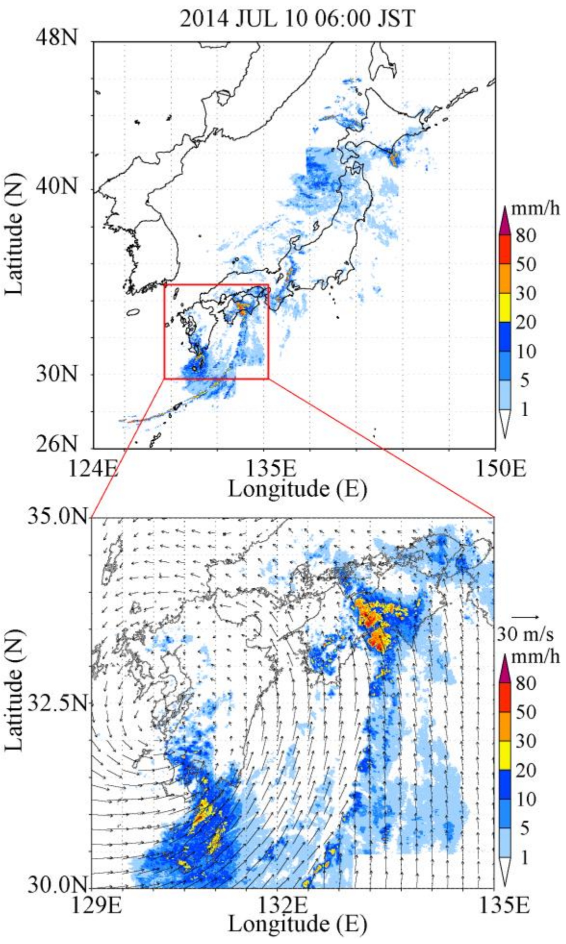

Fig.1 JMA-Radar echo and wind field at 06:00 JST.

**Corresponding author address:* Kochi University, 2-5-1akebono-cho, kochi-shi, Kochi 780-8520 JAPAN; E-mail: sassa@kochi-u.ac.jp

Two tornadoes simultaneously occurred near Kochi airport on 10 July, 2014. At this time, Typhoon, 'Neoguri' located at just west of Kyushu Island and its outer rainband passed through the Kochi Plain as shown in Fig. 1. Though the seashore from Kochi city to Aki city is a hot spot of non-supercell tornadoes (Sassa et al. 2011), we thought possibility that mini supercell may occur in the outer rainband and caused these tornadoes.

The present study aims to clarify the characteristics of parent storm of these tornadoes by analyzing using the data of the JMA radar and the polarimetric radars in Kochi University.

2. ANALYSIS AND DATA

We observed the parent cloud of tornedoes by two polarimetric X-band Doppler radars of Kochi University, Asakura Radar and Monobe Radar, and the Muroto C-band Doppler radar of Japan Meteorological Agency (JMA). As shown in Fig.2, observation ranges of the Monobe, Asakura and JMA-Muroto radars are 30 km, 80 km and 200 km, respectively. We obtained reflectivity and Doppler velocity from PPI scans

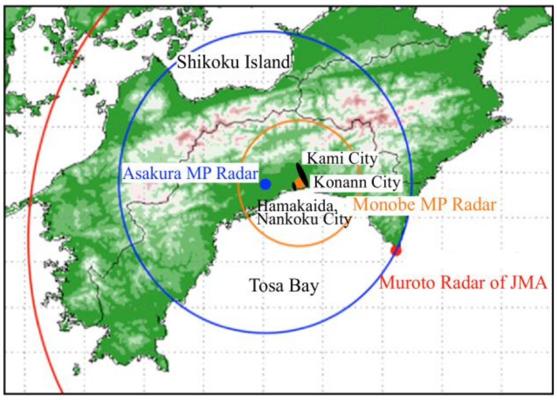

Fig.2 Observation areas of radars. Black ovals indicate the damaged areas.

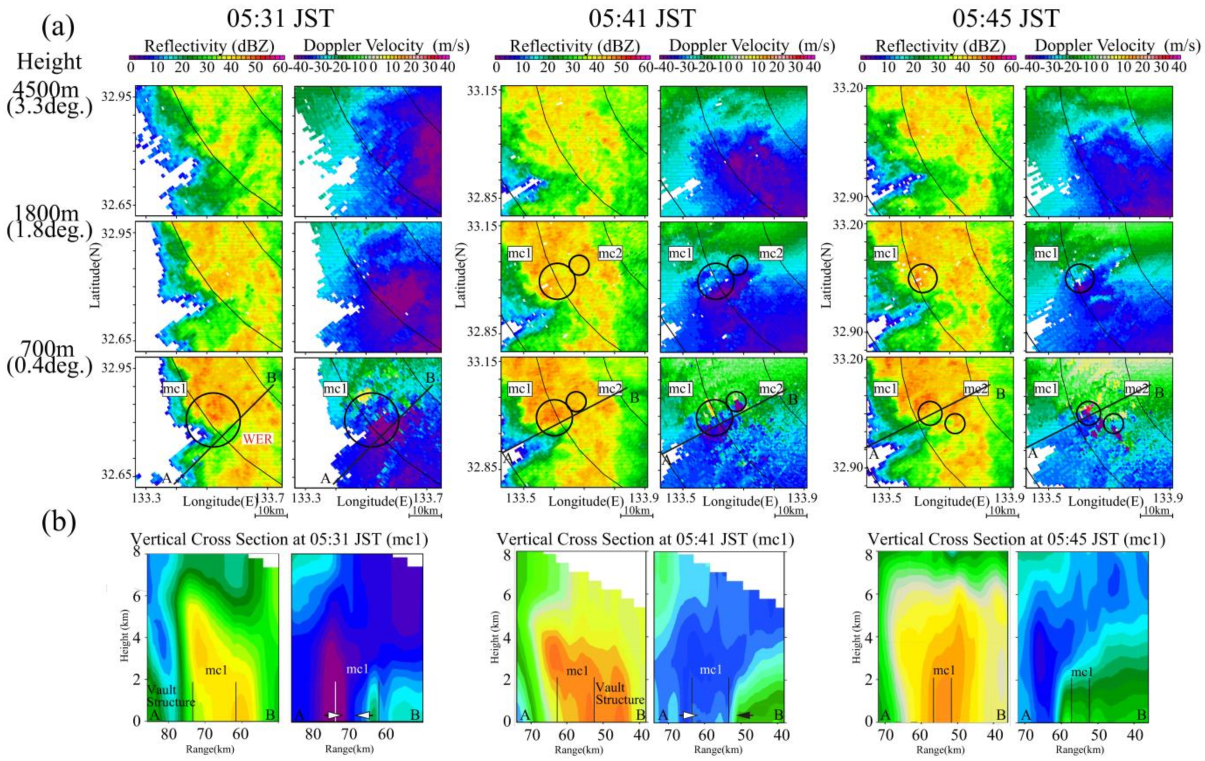

Fig3. JMA-Muroto radar data from 05:31 to 05:45 JST (a) PPI scans (b) Vertical Cross Section.

at lower elevation angles. We also used the initial GPV data of JMA meso scale model archived by Research Institute for Sustainable Humanosphere, Kyoto University.

3. ENVIRONMENTAL CONDITIONS

Environmental parameters in the outer rainband were determined from GPV data. CAPE and SReH were 287 J/kg and 160 m^2/s^2 at 06:00 JST, respectively. These values exceeded the lower limits of environment of supercell genesis, e.g., CAPE = 253 J/kg (McCaul 1987) and SReH = 150 m^2/s^2 (Davies-Jones et al. 1990).

4. RESULTS OF RADAR ANALYSIS

Figure 3 shows the horizontal and vertical cross sections of the parent storm observed by the JMA-Muroto radar. The first mesocyclone, mc1, appeared at 5:31 JST as shown in Fig.3a. The diameter of mc1 was about 10 km. At this time, strong wind of over 38 m/s in Doppler velocity approached to the parent storm from southwest. Weak echo region (WER) was also observed just south side of mc1 and the strong echo than 40 dBZ formed hook like echo pattern around mc1. Moreover, vault structure is clearly observed around mc1 as shown in Fig.3b. These features imply that the parent storm is supercell, but the arrangement of hook echo is opposite to that of ordinary supercell (Lemon and Doswell 1979). The echo top more than 40 dBZ is 5 km. It is almost same as that of the mini-supercell observed in the Kanto Plains, Japan (Suzuki et al. 2000).

Figure 4 shows the Schematic diagram of the parent storm. The parent storm was moving in the outer rainband to the NNE at 27 m/s. For ordinary supercells, warm and moist air mass is supplied from the front right. However, it for the present storm was supplied by strong southwesterly wind conversing to the outer rainband. Namely, the parent storm was generated by strong rear inflow.

Second mesocyclone, mc2, appeared just northeast of mc1 at 5:41JST in Fig.3a. On the other hand, the strong wind approaching to mc1 from southwest became weaken to be 30 m/s.

After this, mc1 rapidly reduced its diameter and vault structure disappeared at 05:45 JST as shown in Fig.3b.

Figure 5 shows some cross sections of the parent storm before and after landfall. Third mesocyclone, mc3, surrounding mc1 appeared at 6:11 JST in Fig.5a. Vault structure was

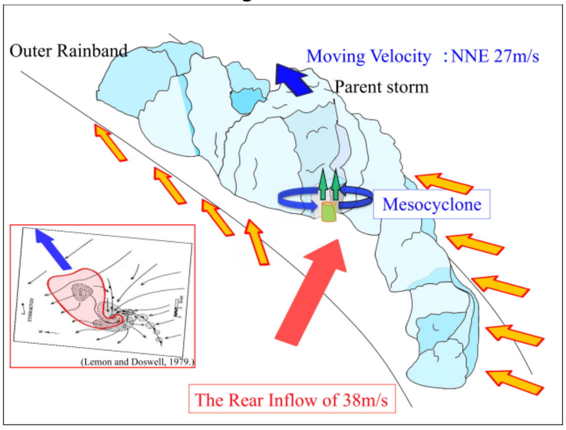

Fig4. Schematic diagram of the parent storm. Red arrow shows the rear inflow. Yellow arrows are the environment wind conversing to the outer rainband. Green arrows are updraft of mesocyclone.

observed in mc3 at 6:15 JST in Fig.5b. Moreover, gust front appeared at the south edge of the parent storm. It moved to the southeast apart from the parent storm. Such situation was different from that of forward flank gust front and/or rear flank gust front of ordinary supercell. After landfall, three vortices still arrived but updraft accompanied by mc3 decayed and divergent flow was observed near ground at 06:21 JST in Fig.5b.

5. TRAJECTORIES

Figure 6 shows the evolution of diameters and the trajectories of the mesocyclones. The mesocyclones, mc1 and mc2 alive for about 1 hour and traveled along the outer rainband. When mc1 appeared at first, its diameter was the largest in its lifetime. And then the diameters of mc1 and mc2 rapidly decreased to be about 1km after the genesis of mc2. These values depend on the resolution of the JMA-Muroto radar. Monobe radar data showed that mc1 and mc2 were misocyclone around

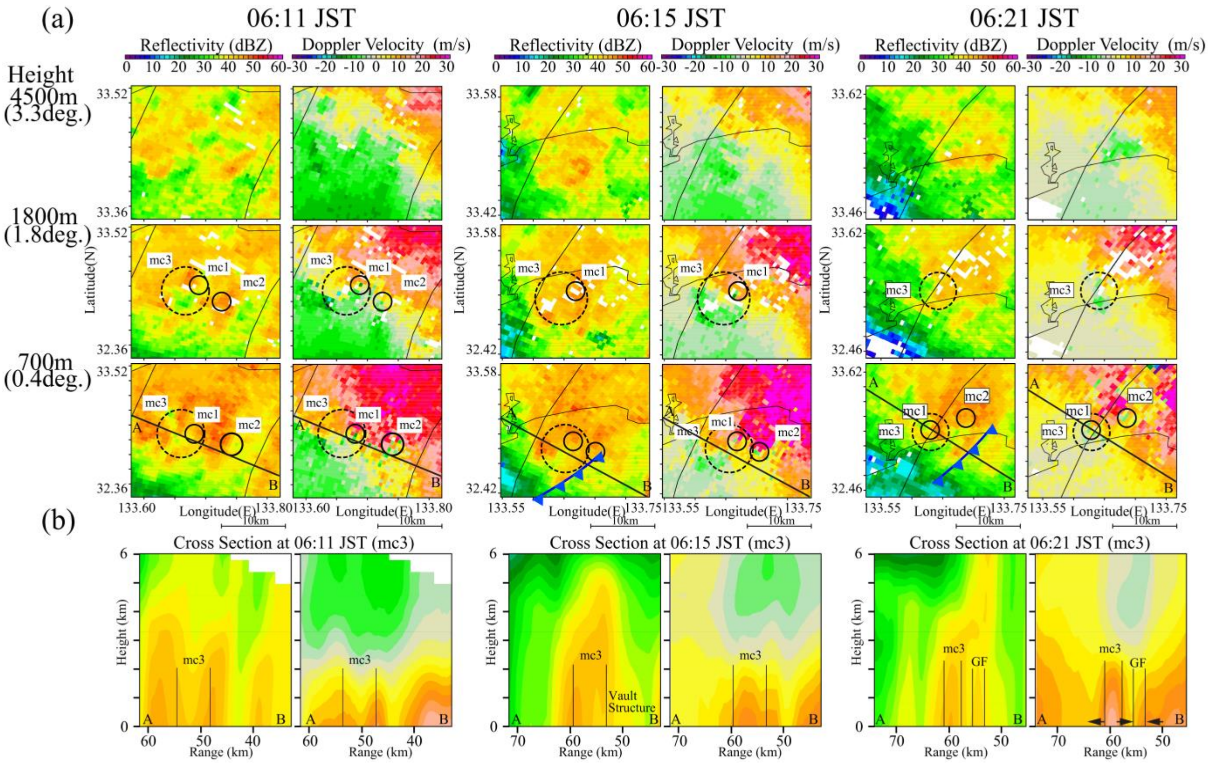

Fig.5 JMA-Muroto radar data from 06:11 to 06:21 JST. (a) PPI scans (b) Cross Section of the mc3. The blue line shows the gust front.

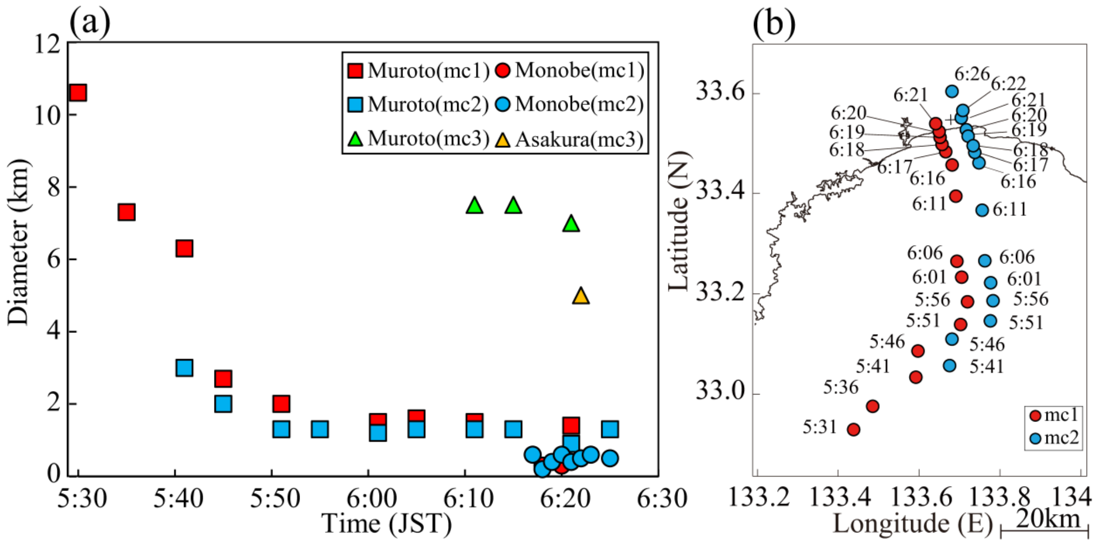

Fig.6 Temporal change of diameter (a) and trajectories (b) of the vortices, mc1, mc2 and mc3.

landfall. These vortices moved northward parallel with each other along the outer rainband. The third mesocyclone, mc3, appeared before landfall. It maybe caused by strong rear inflow intruding the parent storm again. Two tornadoes correspond to mc1 and mc2. Mc1 rapidly disappeared after landfall, whereas the mc2 survived until at 06:26 JST.

6. CONCLUSIONS

The parent storm was founded to have the feature of mini-supercell at the initial stage. But, it was quite different from the ordinary supercell because it generated by strong rear inflow converging to the outer rainband. Such supercell was developed again before landfall. The tornado associated with mc2 survived for several minutes but mc1 and mc3 rapidly decayed after landfall.

ACKNOWLEDGMENTS

This work was supported by JSPS KAKENHI Grant Number 15H02994.

REFERENCES

Davies-Jones, R. P., D. Burgess, and M. Foster, 1990: Test of helicity as a tornado forecast parameter. Preprints, 16th Conf. on Severe Local Storms, Kananaskis Park, AB, Canada, Amer. Meteor. Soc., 588–592.

Lemon, L. R., and C. A. Doswell III, 1979: Severe thunderstorm evolution and mesocyclone structure as related to tornadogenesis. Mon. Wea. Rev., 107, 1184–1197.

Mashiko, W., H. Niino, and T. Kato, 2009: Numerical simulation of tornadogenesis in an outer-rainband minisupercell of Typhoon Shanshan on 17 September 2006. Mon. Wea. Rev., 137, 4238-4260.

McCaul, E. W., Jr., 1987: Observations of the hurricane “Danny” tornado outbreak of 16 August 1985. Mon. Wea. Rev., 115, 1206–1223.

Sassa, K., Y. Hamaguchi, and T. Hayashi, 2011: Characterictices of misocyclones observed on Tosa Bay in Japan. Preprint of 6th European Conference on Severe Storms, Palma de Mallorca, Spain. p.2.

Suzuki, O., H. Niino, H. Ohno, and H. Nirasawa, 2000: Tornado-producing mini supercells associated with Typhoon 9019. Mon. Wea. Rev., 128, 1868–1882.